

See discussions, stats, and author profiles for this publication at: <https://www.researchgate.net/publication/231672950>

# Hydrophobic Protein–Polypyrrole Interactions: The Role of van der Waals and Lewis Acid–Base Forces As Determined by Contact Angle Measurements

ARTICLE in *LANGMUIR* · JANUARY 2002

Impact Factor: 4.46 · DOI: 10.1021/la010444o

CITATIONS

58

READS

48

5 AUTHORS, INCLUDING:



**Ammar Azioune**

Ecole Nationale Supérieure de Biotechnologi...

37 PUBLICATIONS 1,139 CITATIONS

SEE PROFILE



**Mohamed Chehimi**

Institut de Chimie et des Matériaux Paris-Est

269 PUBLICATIONS 5,397 CITATIONS

SEE PROFILE



**Beata Miksa**

Centre of Molecular and Macromolecular Stu...

29 PUBLICATIONS 407 CITATIONS

SEE PROFILE



**Teresa Basinska**

Centre of Molecular and Macromolecular Stu...

39 PUBLICATIONS 547 CITATIONS

SEE PROFILE

# Hydrophobic Protein–Polypyrrole Interactions: The Role of van der Waals and Lewis Acid–Base Forces As Determined by Contact Angle Measurements

Ammar Azioune,<sup>†</sup> Mohamed M. Chehimi,<sup>\*,†</sup> Beata Miksa,<sup>‡</sup> Teresa Basinska,<sup>‡</sup> and Stanislaw Slomkowski<sup>‡</sup>

*Interfaces, Traitement, Organisation et Dynamique des Systèmes (ITODYS), Université Paris 7—Denis Diderot, Associé au CNRS (UMR 7086), 1 Rue Guy de la Brosse, 75005 Paris, France, and Center of Molecular and Macromolecular Studies, Polish Academy of Science, Sienkiewicza 112, Łódź 90-363, Poland*

Received March 26, 2001. In Final Form: October 21, 2001

Adsorption of human serum albumin (HSA) onto conducting polypyrrole powders, doped with chloride (PPyCl), dodecyl sulfonate (PPyDS), and tosylate (PPyTS), has been monitored in 0.1 M phosphate buffer saline (PBS) and pH 7.4 using UV–visible spectroscopy in conjunction with the depletion method. The decreasing trend of adsorption was PPyTS > PPyDS > PPyCl and was interpreted in terms of hydrophobic interactions. Electrochemically synthesized PPyCl, PPyDS, and PPyTS films were used as model surfaces for contact angle measurements. Both static, advancing, and receding water contact angle ( $\theta_w$ ) suggested that the PPyTS is the most hydrophobic polymer among the three under test. The simple measure of  $\theta_w$  permitted qualitative interpretation of the adsorption trend in terms of hydrophobic protein–PPy interactions. The van Oss–Good–Chaudhury (VOGC) method was further used to determine the dispersive, acidic, and basic components of the surface free energy ( $\gamma_s^d$ ,  $\gamma_s^+$ , and  $\gamma_s^-$ , respectively) of the conducting polypyrroles. These components show that polypyrrole generally behaves as a strong Lewis acid. The three surface free energy components were subsequently used to assess the absolute hydrophobicity of the substrates ( $\Delta G_{1W1}$ ), that is, the PPy–PPy interaction in water, the trend of which is that of protein adsorption. More importantly, the VOCG theory permitted determination of  $\Delta G_{1W2}$ , the free energy of protein–PPy in water, that is, the extent of hydrophobic interaction forces. The decreasing trend of  $\Delta G_{1W2}$  values (absolute) was found to be PPyTS > PPyDS > PPyCl. This is a quantitative evidence for the role of hydrophobic interactions at the protein–PPy interface. In the case of PPyTS and PPyDS, the acid–base force contribution was much more important than the van der Waals one. In contrast, for the HSA–PPyCl system, the van der Waals forces predominantly contributed to  $\Delta G_{1W2}$ .

## Introduction

Protein adsorption onto (polymeric) surfaces is very actively studied for the development biomaterials, biological assays, and biosensors in addition to the fundamental research on its driving mechanisms.<sup>1–7</sup> This process occurs whenever an aqueous solution of protein comes into contact with a solid surface. The protein diffuses to the surface where it will adsorb and form strong bonds with specific sites on the surface. However, this seemingly simple process can in reality be extremely complicated and, despite numerous investigations, is still not completely understood.<sup>8</sup>

For example, attempts were made to understand the adsorption process by investigating the molecular con-

tributions to the adsorption process, such as hydrophilic/hydrophobic interactions at interfaces. The primary driving force of protein adsorption seems to be the hydrophobic interactions.<sup>9–11</sup> Electrostatic contributions play an important role as well, particularly for the more hydrophilic surfaces.<sup>12–16</sup> In addition, surface geometry and the topography considerations are likely to play a role. This is especially true for the complex solid surfaces such as block copolymers. The protein adsorption is influenced in this case by the conformational changes due to the topography and the hydrophobicity of the surfaces.<sup>17,18</sup> There are other contributions to protein adsorp-

<sup>†</sup> Université Paris 7—Denis Diderot (CNRS (UMR 7086)).

<sup>‡</sup> Polish Academy of Science.

(1) Andrade, J. D.; Hlady, V. *Adv. Polym. Sci.* **1987**, *79*, 1.

(2) Lee, J. S.; Nakahama, S.; Hirao, A. *Sens. Actuators, B* **1991**, *3*, 215. Prusak-Sochaczewski, E.; Luong, J. H. T. *Anal. Lett.* **1990**, *23*, 401. Harsányi, G., Ed. *Polymer Films in Sensor Applications*; Technomic Publishing Co., Inc.: Lancaster, PA, 1995.

(3) Elgersma, A. V.; Zsom, R. L. J.; Norde, W.; Lyklema, J. *J. Colloid Interface Sci.* **1990**, *138*, 145.

(4) Ladam, G.; Schaaf, P.; Cuisinier, F. J. G.; Decher, G.; Voegel, J.-C. *Langmuir* **2001**, *17*, 878.

(5) Wälivaara, B.; Askendal, A.; Lundström, I.; Tengvall, P. *J. Colloid Interface Sci.* **1997**, *187*, 121. McMaster, T. J.; Miles, M. J.; Shewry, P. R.; Tatham, A. S. *Langmuir* **2000**, *16*, 1463.

(6) Chapman, R. G.; Ostuni, E.; Liang, M. N.; Meluleni, G.; Kim, E.; Yan, L.; Pier, G.; Shaw Warren, H.; Whitesides, G. M. *Langmuir* **2001**, *17*, 1225.

(7) Basinska, T.; Slomkowski, S.; Dworak, A.; Panchev, I.; Chehimi, M. M. *Colloid Polym. Sci.* **2001**, *279*, 916.

(8) Nadarajah, A.; Lu, C. F.; Chittur, K. K. Modeling the Dynamics of Protein Adsorption to Surfaces. In *Proteins at Interfaces II*; Thomas, A., Horbett, Brash, J. L., Eds.; ACS Symposium; American Chemical Society: Washington, DC, 1995; p 181.

(9) Schmaier, A. H.; Silver, L.; Adams, A. L.; Fischer, T. C.; Munoz, P. C.; Colman, R. W. *Thromb. Res.* **1983**, *33*, 51.

(10) Wojciechowski, P.; Ten Hore, P.; Brash, J. L. *J. Colloid Interface Sci.* **1986**, *111*, 455.

(11) Slack, S. M.; Horbett, T. A. *J. Colloid Interface Sci.* **1989**, *133*, 148.

(12) Norde, W. In *Surfaces and Interfacial Aspects of Biomedical Polymers*; Andrade, J. D., Ed.; Plenum Press: New York, **1985**; Vol. 2.

(13) Kondo, A.; Higashitani, K. *J. Colloid Interface Sci.* **1992**, *150*, 344.

(14) Shibata, C. T.; Lenhoff, A. M. *J. Colloid Interface Sci.* **1994**, *148*, 469.

(15) Nylander, T.; Kékicheff, P.; Ninham, B. W. *J. Colloid Interface Sci.* **1994**, *164*, 136.

(16) Horsley, D.; Herron, J.; Hlady, V.; Andrade, J. D. *Langmuir* **1991**, *7*, 218.

(17) Lu, D. R.; Park, K. *J. Colloid Interface Sci.* **1991**, *144*, 271.

(18) Israelachvili, J. N.; Pashley, R. M. *J. Colloid Interface Sci.* **1984**, *98*, 500.

tion, such as those due to the van der Waals forces, but they are known to be much smaller in magnitude.<sup>18,19</sup> Investigations on the role of molecular forces governing protein adsorption were mainly conducted in the case of classical materials such as metals, minerals, and polymers.<sup>20</sup>

In the past 2 decades, conducting polypyrrole has attracted much attention, mainly because of its relatively high environmental stability,<sup>21</sup> electrical properties,<sup>22</sup> ion-exchange capacity,<sup>23</sup> and its biocompatibility.<sup>24</sup> Polypyrrole has unique properties such as redox chemistry and conductivity that make it suitable for the design of novel biosensors.<sup>25,26</sup> In addition, this conducting polymer has an intrinsic deep black color very useful for visual immunodiagnoses tests.<sup>27,28</sup> As far as the latter application is concerned, Pope et al.<sup>28</sup> have shown that protein adsorption rather than covalent grafting can be sufficient for the development of a new assay using polypyrrole-based material as a carrier for the antibody. Of relevance to the present paper, protein adsorption studies on conducting polymers were reported in the literature. HSA has been adsorbed onto polypyrrole core/polyacrolein shell latex up to 11 mg/g.<sup>29</sup>

Adsorption of BSA and alkaline phosphatase onto chloride-doped polypyrrole (PPyCl) was found to be pH-dependent.<sup>30</sup> Smith and Knowles<sup>31</sup> studied the influence of the polypyrrole conductivity on protein binding as a function of pH. They showed that the conductivity of polypyrrole depended on the pH of the medium, but the ability to bind protein did not show any such variation.

As far as the Paris group is concerned, adsorption measurements of biological macromolecules were performed using polypyrrole powders and polypyrrole colloidal particles as substrates. Polypyrrole powder was found to be a fairly strong bioadsorbent of DNA fragments.<sup>32</sup> Electrostatic interactions were found to be the driving forces for the DNA–polypyrrole interactions since DNA is negatively charged and polypyrrole positively charged. Adsorption was favored on the polypyrrole–silica nanocomposites which bear positive charges at the surfaces or strongly hydrogen bonding functional groups. We extended our adsorption studies of biological macromolecules to proteins using human serum albumin (HSA) as a model one. In preliminary experiments,<sup>33</sup> adsorption of HSA was

carried out onto polypyrrole powder and polypyrrole–silica nanocomposite at pH 7.4 and room temperature. Using UV spectroscopy, we found that the nanocomposite was more effective than the powder in adsorbing HSA (147 and 63 mg/g, respectively). It is worth noting that polypyrrole–silica is adsorptive toward HSA at pH 7.4 by contrast with the quasi zero adsorption we previously obtained with the DNA adsorbate.<sup>34</sup>

X-ray photoelectron spectroscopy (XPS) was also used for a direct characterization of HSA at the surface of polypyrrole. This specific surface analytical technique was further employed to construct adsorption isotherms of HSA, which were found to be of the high-affinity type thus confirming the rather indirect depletion method.

The objectives of this paper are as follows:

(i) Determination of adsorption isotherms of HSA onto polypyrrole powders doped with various anions using the Lowry method.<sup>35</sup>

(ii) Understanding the type of molecular forces which govern the protein–polypyrrole interactions.

(iii) Determination of the surface free energy and its dispersive, acidic, and basic components of PPy films by means of contact angle measurements of reference liquids (to characterize polypyrrole by contact angle measurements using the sessile drop technique, we have electrochemically synthesized thin PPyCl, PPyDS (polypyrrole powder doped with dodecyl sulfonate) and PPyTS (polypyrrole powder doped with tosylate) films; this form of material is much more amenable to wettability measurements than powders).

(iv) Attempt to relate the adsorptive capacity of polypyrrole toward HSA to the surface thermodynamics properties (van der Waals and acid–base) of the substrates (in this regard, the van Oss–Good–Chaudhury (VOGC) theory<sup>36</sup> of surface tension components will be used to calculate the free energy of interactions between polypyrrole and protein in water, that is, the strength of hydrophobic interactions between the polymer and the protein).

### Theory of van der Waals and Acid–Base Interactions in Wetting and Adhesion

The thermodynamic work of adhesion  $W$  is by definition the free energy change per unit area required to separate to infinity two surfaces initially in contact with a result of creating two new surfaces. In the absence of chemisorption and interdiffusion,  $W$  is the sum of the various intermolecular forces involved and can be related to the surface free energies (Dupré's equation):

$$W = \gamma_1 + \gamma_2 - \gamma_{12} \quad (1)$$

where  $\gamma_1$  and  $\gamma_2$  are the surface free energies of components 1 and 2 and  $\gamma_{12}$  is the interfacial free energy. In 1964, Fowkes<sup>37</sup> proposed that both the reversible work of adhesion ( $W$ ) and the surface tension ( $\gamma$ ) had additive components:

$$W = W^d + W^p + W^h + W^m \dots$$

$$\gamma = \gamma^d + \gamma^p + \gamma^h + \gamma^m \dots$$

where d, p, h, and m refer to dispersion forces, dipole

(19) Jeon, S. I.; Lee, J. H.; Andrade, J. D.; P. G. de Gennes, *J. Colloid Interface Sci.* **1992**, *142*, 149.

(20) *Proteins at Interfaces II, Fundamentals and Applications*; Horbett, T. A., Ed.; American Chemical Society: Washington, DC, **1995**.

(21) Street, G. B. In *Handbook of Conducting Polymers*; Skotheim, T. A., Ed.; Dekker: New York, **1986**; Vol. 1, p 265.

(22) Garnier, F. *La Recherche* **1987**, *18*, 1306.

(23) Hailin, G.; Wallace, G. G. *Anal. Chem.* **1989**, *61*, 198.

(24) Bidan, G. In *Propriétés Électriques des Polymères et Applications*; Groupe Français d'Études et Applications des Polymères, Ed.; **1993**.

(25) Barnett, D.; Liang, D. G.; Skopec, S.; Sadik, O.; Wallace, G. G. *Anal. Lett.* **1994**, *27*, 2417.

(26) Tarcha, P. J.; Misun, D.; Fineley, D.; Wong, M.; Donovan, J. J. In *Polymer Latexes. Preparation, Characterization and Applications*; Daniels, E. S., Sudol, E. D., El-Aasser, M. S., Eds.; ACS Symposium Series 492; American Chemical Society: Washington, DC, **1992**; pp 347–367.

(27) Tarcha, P. J.; Donovan, J. J.; Wong, M. Indicator reagents, diagnostic assays and test kits employing organic polymer latex particles. U. S. Pat. 5,252,459, 1993.

(28) Pope, M. R.; Armes, S. P.; Tarcha, P. J. *Bioconjugate Chem.* **1996**, *4*, 436.

(29) Miksa, B.; Slomkowski, S. *Colloid Polym. Sci.* **1995**, *273*, 47.

(30) Smith, A. B.; Knowles, C. J. *Biotechnol. Appl. Biochem.* **1990**, *12*, 661.

(31) Smith, A. B.; Knowles, C. J. *J. Appl. Polym. Sci.* **1991**, *43*, 399.

(32) Saoudi, B.; Jammul, N.; Abel, M. L.; Chehimi, M. M.; Dodin, G. *Synth. Met.* **1997**, *87*, 97.

(33) Azioune, A.; Pech, K.; Saoudi, B.; Chehimi, M. M.; McCarthy, G. P.; Armes, S. P. *Synth. Met.* **1999**, *102*, 1419.

(34) Saoudi, B.; Jammul, N.; Chehimi, M. M.; McCarthy, G. P.; Armes, S. P. *J. Colloid Interface Sci.* **1997**, *192*, 269.

(35) (a) Lowry, D. H.; Rosenbrough, N. J.; Farr, A. L.; Randall, R. J. *J. Biochem.* **1951**, *193*, 265. (b) Slomkowski, S.; Basinska, T. In *Polymer Latexes. Preparation, Characterization and Applications*; Daniels, E. S., Sudol, E. D., El-Aasser, M. S., Eds.; ACS Symposium Series 492; American Chemical Society: Washington, DC, **1992**; pp 328–346.

**Table 1.** Surface Tension Components (mJ/m<sup>2</sup>) for Commonly Used Test Liquids<sup>39</sup>

liquids	$\gamma$	$\gamma^d$	$\gamma^{AB}$	$\gamma^+$	$\gamma^-$
water	72.8	21.8	51	25.5	25.5
glycerol	64	34	30	3.92	57.4
Formamide	58	39	19	2.28	39.6
$\alpha$ -bromonaphthalene	44.4	43.5	0	0	0
CH <sub>2</sub> I <sub>2</sub>	50.8	50.8	0	0	0

interactions, hydrogen bonding (a subset of Lewis acid–base interactions), and metallic bonding, respectively.

For two materials interacting via London dispersive forces only across their interface, Fowkes<sup>37</sup> suggested that  $W$  be described by

$$W = W^d = 2(\gamma_1^d \gamma_2^d)^{1/2} \quad (2)$$

where  $W^d$  is the dispersive contribution to the work of adhesion and  $\gamma_i^d$ , the dispersive contribution to the surface energy  $\gamma_i$ . If material 1 is acidic (basic) and material 2 basic (acidic), they can interact via acid–base forces and  $W$  can be described by

$$W = W^d + W^{AB} \quad (3)$$

where  $W^{AB}$  is the acid–base contribution to  $W$ . Combining eqs 2 and 3 leads to

$$W^{AB} = W - 2(\gamma_1^d \gamma_2^d)^{1/2} \quad (4)$$

van Oss et al.<sup>36</sup> introduced the notion of acidic and basic components to the surface energy ( $\gamma^+$  and  $\gamma^-$ , respectively) to characterize the acid–base properties of materials and predict  $W^{AB}$ :

$$W^{AB} = 2(\gamma_1^+ \gamma_2^-)^{1/2} + 2(\gamma_1^- \gamma_2^+)^{1/2} \quad (5)$$

$\gamma^+$  and  $\gamma^-$  for a solid can be determined by contact angle measurements using three reference liquids of known  $\gamma_L^d$ ,  $\gamma_L^+$ , and  $\gamma_L^-$  (see Table 1). The acidic and basic surface tension components for test liquids were established with model surfaces and liquids on the assumption that for water  $\gamma_L^- = \gamma_L^+ = 25.5$  mJ/m<sup>2</sup> and

$$\gamma_L^{AB} = 2(\gamma_L^+ \gamma_L^-)^{1/2} \quad (6)$$

Numerical application of eq 6 to water (w) yields

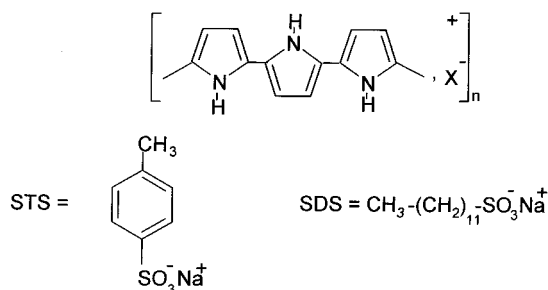
$$\gamma_w^{AB} = 2(25.5 \times 25.5)^{1/2} = 51 \text{ mJ/m}^2$$

The surface tension components of solid surfaces can be determined by contact angle measurements of reference liquids. The wetting of a solid surface by a liquid drop is expressed by Young's equation:

$$\gamma_S - \gamma_{SL} = \gamma \cos \theta \quad (7)$$

Combining (7) and (1), one obtains the Young–Dupré equation of the work of adhesion:

$$W_a = \gamma(1 + \cos \theta) \quad (8)$$

**Chart 1.** Structure of Polypyrrole Showing One Anion Dopant ( $X^-$ ) per Three Pyrrole Repeat Units Bearing One Positive Charge Altogether (in This Case the Doping Level Would Be 33.3%)

Combining and rearranging eqs 8, 2, and 5 results in

$$\gamma_L(1 + \cos \theta) = 2(\gamma_S^d \gamma_L^d)^{1/2} + 2(\gamma_S^+ \gamma_L^-)^{1/2} + 2(\gamma_S^- \gamma_L^+)^{1/2} \quad (9)$$

where  $\theta$  is the only measurable datum and  $\gamma_S^d$ ,  $\gamma_S^+$ , and  $\gamma_S^-$  are the unknowns. The latter can be determined using at least three test liquids of known surface tension components. Therefore, the total surface free energy of the solid surface can be determined by

$$\gamma_S = \gamma_S^d + 2(\gamma_S^+ \gamma_S^-)^{1/2} = \gamma_S^d + \gamma_S^{AB} \quad (10)$$

where  $\gamma_S^{AB}$ , the overall acid–base contribution to  $\gamma_S$ , is evaluated as in eq 6.

## Experimental Section

**Synthesis of PPy Powders.** Pyrrole (1.00 mL, Acros) was purified under a column of silica prior to polymerization and then was added via pipettman to 100 mL of a stirred aqueous solution of  $FeCl_3 \cdot 6H_2O$  (9.74 g, Aldrich) at room temperature. The mixture was stirred overnight. The resulting black precipitate was vacuum-filtrated and thoroughly washed with deionized water and ethanol. The powder was then dried in a desiccator overnight and sieved (180  $\mu$ m) before adsorption. The resulting powder was PPyCl. The PPyDS and PPyTS were synthesized under the same procedure, with addition of 1.41 g of sodium dodecyl sulfate and 0.982 g of sodium *p*-toluene sulfonate to the  $FeCl_3 \cdot 6H_2O$  solution. The structure of the polypyrrole powder particles is shown in Chart 1.

**Synthesis of PPy Films.** The electrosynthesis of doped PPy films took place in a one-compartment cell containing 0.1 M of pyrrole and an aqueous supporting electrolyte solution of 0.1 M of salts (sodium chloride, sodium dodecyl sulfate, and sodium tosylate). The solutions were adjusted to approximately pH = 7 prior polymerization. The PPy films were deposited galvanostatically onto 12  $\times$  12 mm platinum-coated glass slides at a current density of 0.4 mA/cm<sup>2</sup>. Under these conditions, the thickness of the PPy films was estimated to 100 nm and the average roughness is expected to be less than 5 nm.<sup>38</sup> The electrodes were rinsed after polymerization with ethanol.

**Protein Adsorption.** A 10 mg amount of PPy powders were immersed in 10 mL of PBS (0.1M and pH 7.4) and stirred overnight for ion-exchange. The suspension was then centrifuged to separate the conditioned solid particles. The conditioned PPy particles were introduced in 10 mL of phosphate buffer saline (PBS) solutions of HSA (Sigma product, fraction Cohen V). We applied the "one-shot" method with initial protein concentration varying from 10 to 500  $\mu$ g/mL. Incubation was carried out overnight in glass tubes. Gentle stirring of the polypyrrole suspension in HSA solutions was performed overnight using a

(36) van Oss, C. J.; Good, R. J.; Chaudhury, M. K. *Langmuir* **1988**, 4, 884.

(37) Fowkes, F. M. *Ind. Eng. Chem.* **1964**, 56, 40.

(38) Abel, M. L.; Camalet, J.-L.; Chehimi, M. M.; Watts, J. F.; Zhdan, P. A. *Synth. Met.* **1996**, 81, 23.

(39) Good, R. J.; Chaudhury, M. K.; van Oss, C. J. In *Fundamentals of Adhesion*; Lee, L. H. Ed.; Plenum Press: New York, 1991; Chapter 4.



Table 2. Contact Angles of Reference Liquid Drops on Polypyrrole Film Surfaces

	water			glycerol	formamide	CH <sub>2</sub> I <sub>2</sub>	$\alpha$ -bromonaphthalene
	static	advancing	receding				
PPyCl	52.8 $\pm$ 3.2	<i>a</i>	24 $\pm$ 5	54.1 $\pm$ 1.5	43.8 $\pm$ 2.2	<i>a</i>	<i>a</i>
PPyDS	69.1 $\pm$ 5.9	59 $\pm$ 3	43.1 $\pm$ 6.9	64.8 $\pm$ 5.2	43.9 $\pm$ 1.1	49 $\pm$ 4	24.5 $\pm$ 4.5
PPyTS	80 $\pm$ 5	76.6 $\pm$ 4.4	49 $\pm$ 6	67.6 $\pm$ 2.4	54.8 $\pm$ 1.2	44 $\pm$ 2	30.3 $\pm$ 0.7

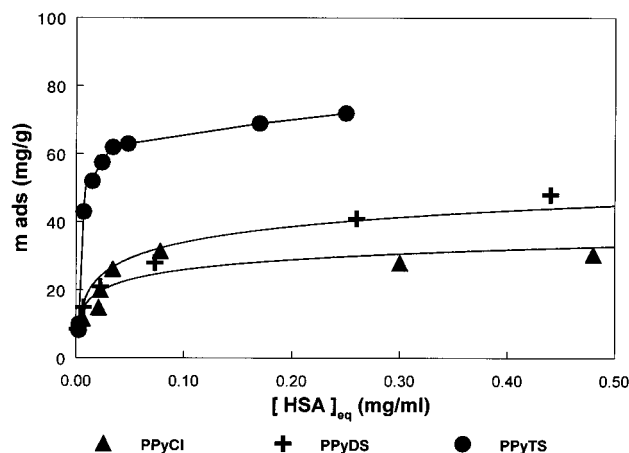
<sup>a</sup> Spreading.

Figure 1. Adsorption isotherms of HSA onto PPyCl, PPyDS, and PPyTS at 0.1 M PBS and pH 7.4.

Speci-Mix apparatus. After incubation, the suspension was centrifuged for the second time, and HSA concentration in the supernatant was determined by the Lowry method using UV–visible spectroscopy.<sup>35</sup> The amount of protein adsorption was calculated from the depletion method as follow:

$$M = (C_i - C_0) V_{\text{soln}} / m_{\text{PPy}}$$

where  $M$  is the amount of adsorbed HSA (mg/g) and  $C_i$  and  $C_0$  represent initial and equilibrium HSA concentrations (mg/mL), respectively.  $V_{\text{soln}}$  is the total volume solution (mL), and  $m_{\text{PPy}}$  is the amount of PPy powder (g).

**Contact Angle Measurements.** Liquid contact angles were measured using a RAME HART NRL goniometer (model 100-00) equipped with a microscope and illumination system to visualize both the drop deposited on the plates and the measurement marker. The plates were placed on a flat, horizontal support in a chamber which was thermostated at 20 °C.

Contact angles from both ends (left and right) were considered and usually found equal within standard error. Static, advancing, and receding contact angles were determined. Drops of 2–3  $\mu$ L of liquids were used to determine static contact angles. Advancing contact angles were obtained by adding an extra 2  $\mu$ L to the drop already in contact with the surface. In contrast, receding contact angles were obtained by sucking 1–2  $\mu$ L from the initial drop. Static contact angles were the average values of at least six measurements.

The list of reference liquids used to characterize the polypyrrole surface is reported in Table 1 together with their surface tension components.

## Results and Discussion

**(1) Protein Adsorption Isotherms onto Polypyrrole Powders.** Adsorption isotherms were obtained by plotting the amount of adsorbed HSA (mg/g) versus the equilibrium HSA concentration (Figure 1). HSA experiences a massive adsorption onto polypyrrole in the range of 25–70 mg/g. However, the maximum of adsorption depends on the polypyrrole nature, thus on the dopant nature, a result that we have previously obtained in the case of DNA fragments<sup>32</sup> and preliminary HSA adsorption studies.<sup>33</sup> In the present work, the PPyTS substrate is much more adsorptive toward HSA than PPyDS and PPyCl.

The shape of the isotherms indicates that they are of the high-affinity type and fit the Langmuir model, indicating that the adsorption energy of one protein molecule is not affected by that of another already at the surface. This contrasts with the cooperativity of DNA fragments when they adsorb on polypyrrole powders.<sup>32</sup>

Since adsorption was carried at a pH higher than the HSA isoelectric point (IEP = 4.8), most probably electrostatic interactions play an important role due to the positively charged polypyrrole chains and the net negative charge of HSA at pH 7.4, a situation similar to that recently reported by Ladam et al.<sup>4</sup> for proteins bearing opposite charge to that of the polymeric sorbent. These electrostatic interactions are more operative at long range.<sup>40</sup> One can then consider the hydrophobic interactions between HSA and polypyrrole to interpret the adsorption differences. One thus must investigate the hydrophilic/hydrophobic properties of the substrate using water contact angles or by applying the more elegant VOGC theory<sup>36</sup> to wettability data in order to determine surface tension components and subsequently interfacial interaction energies.

**(2) Liquids Contact Angles on Polypyrrole Surfaces and Relation to Adsorption.** The contact angle data are reported in Table 2. We have implemented the data corresponding to receding ( $\theta_r$ ) and advancing ( $\theta_{\text{adv}}$ ) contact angles of water as well. We have also performed measurement of  $\theta_r$  and  $\theta_{\text{adv}}$  and found that usually  $\theta_r < \theta$ . A few  $\theta_{\text{adv}}$  were determined, and they were usually as large or larger than the static angles. However,  $\theta_r$  and  $\theta_{\text{adv}}$  for the various liquids (except water) were too scattered and are thus of limited use.

CH<sub>2</sub>I<sub>2</sub> and  $\alpha$ -bromonaphthalene spread spontaneously on PPyCl, whereas a contact angle of  $40.6 \pm 1^\circ$  has been reported for the former liquid wetting a PPyCl film.<sup>41</sup>

Table 2 shows, on the basis of water contact angles, that the decreasing hydrophobicity trend is PPyTS > PPyDS > PPyCl, and this is either using static or receding contact angles. The static water contact angle on PPyCl is comparable to  $57.5 \pm 1.1$ .<sup>41</sup>

Advancing contact angles of water are surprisingly slightly smaller than  $\theta$ . This may be due to a slight increase of the contact area of the water drop when performing advancing angle measurements, thus leading to a reverse situation of lower contact angle rather than higher.<sup>42</sup> We have related the amount of adsorbed protein to  $\theta_r$  for water drops deposited on polypyrrole films. Figure 2 shows that adsorption increased with water receding contact angles, that is, with the hydrophobic character of the polypyrrole films. The trends of the maximum adsorption vs  $\theta$  and  $\theta_r$  are the same, but the choice of  $\theta_r$  to plot the graph in Figure 2 was dictated by the fact that it will describe wetting at the retreat of water better than the static angle.

Of course the use of  $\theta$  and  $\theta_r$  is not sufficient to characterize fully the hydrophobic character of surfaces.

(40) Israelachvili, J. *Intermolecular Surface Forces*, 2nd ed.; Academic Press: London, 1992.

(41) Liu, M. J.; Tzou, K.; Gregory, R. V. *Synth. Met.* **1993**, *63*, 67.

(42) Zenkiewicz, M., Ed. *Adhezja i Modyfikowanie Warstwy Wierzchniej Tworzyw Wielkocząsteczkowych*, Wydawnictwa Naukowo-Techniczne (ISBN 83-204-2547-6): Warsaw, Poland, 2000; Chapter 3, pp 75–126.

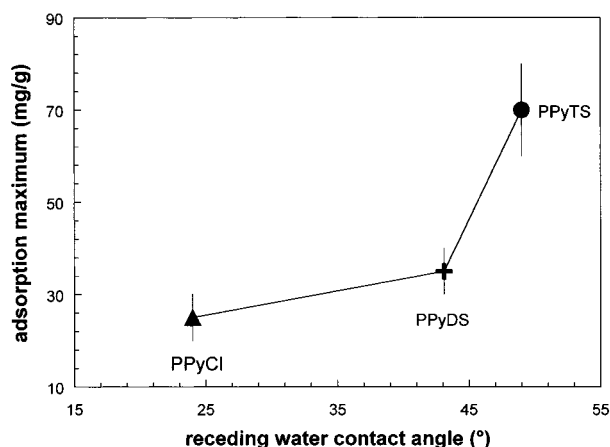


**Figure 2.** Plot of the maximum of HSA adsorption vs receding contact angles of water drops on PPyCl, PPyDS, and PPyTS.

A more thorough determination of the hydrophobic character of the substrates and hydrophobic interactions with proteins in water can be achieved using the VOGC theory of interfacial interaction energies.<sup>43</sup> This requires more probe liquids of known  $\gamma_L^d$ ,  $\gamma_L^+$  and  $\gamma_L^-$  components. The reference liquid characteristics together with the contact angle data will permit assessment of the surface free energy of the materials under test (that is, dispersive, acidic, and basic components of  $\gamma_S$ ).

**(3) Determination of the Surface Tension Components.** Equation 9 was used to estimate the surface tension component for PPyCl, PPyDS, and PPyTS. However, the problem can be solved in two steps. First,  $\gamma_S^d$  can be determined using an apolar liquid (e.g.  $\text{CH}_2\text{I}_2$  or  $\alpha$ -bromonaphthalene) for which  $\gamma_L = \gamma_L^d$ . In this case, eq 9 reduces to

$$\gamma_L(1 + \cos \theta) = 2(\gamma_S^d \gamma_L^d)^{1/2} \quad (11)$$

Two unknowns are yet to be determined for the solid material following rearrangement of eq 9:

$$\gamma_L(1 + \cos \theta) - 2(\gamma_S^d \gamma_L^d)^{1/2} = 2(\gamma_S^+ \gamma_L^-)^{1/2} + 2(\gamma_S^- \gamma_L^+)^{1/2} \quad (12)$$

To do so, one can use water and  $n$  ( $n \geq 1$ ) other monofunctional (pure acid or base) or bifunctional (amphoteric) liquids of which  $\gamma_L^+$  and/or  $\gamma_L^-$  are  $>0$  mJ/m<sup>2</sup>. One can graphically determine  $\gamma_S^+$  and/or  $\gamma_S^-$  using a rearrangement of (12):

$$[\gamma_L(1 + \cos \theta) - 2(\gamma_S^d \gamma_L^d)^{1/2}]/2(\gamma_L^-)^{1/2} = (\gamma_S^+)^{1/2} + (\gamma_S^-)^{1/2}(\gamma_L^+/\gamma_L^-)^{1/2} \quad (13)$$

The left-hand side of eq 13 equals  $W^{AB}/2(\gamma_L^-)^{1/2}$  (see eq 5). For a series of monofunctional and/or bifunctional test liquids used, one can plot  $W^{AB}/2(\gamma_L^-)^{1/2}$  versus  $(\gamma_L^+/\gamma_L^-)^{1/2}$ .<sup>44</sup> This leads to a linear correlation with  $(\gamma_S^+)^{1/2}$  and  $(\gamma_S^-)^{1/2}$  as intercept and slope, respectively. Graphical application of this simple approach is shown in Figure 3 for PPys substrates and poly(methyl methacrylate) (PMMA) using the contact angle data reported in Table 2 for the

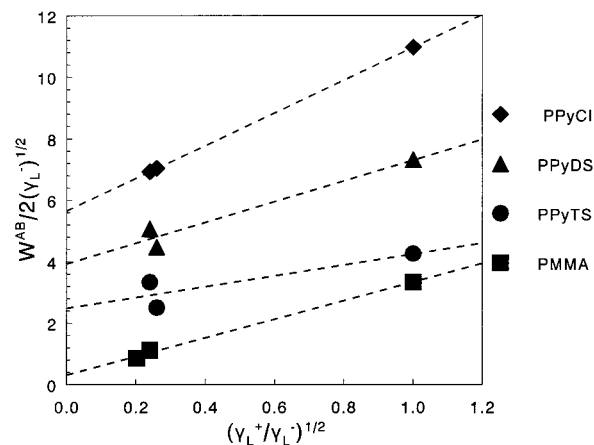


**Figure 3.** Plot of  $W^{AB}/2(\gamma_L^-)^{1/2}$  vs  $(\gamma_L^+/\gamma_L^-)^{1/2}$ : a graphical determination of electron acceptor and electron donor constants ( $\gamma_S^+$ ,  $\gamma_S^-$ ) for PPyCl, PPyDS, PPyTS, and PMMA. The contact angle data for PMMA were taken from ref 45. For clarity, the y-axis values of the conducting polymers were increased by 5, 3, and 1 units (mJ<sup>1/2</sup>/m) for PPyCl, PPyDS, and PPyTS, respectively.

conducting polymers and by Good and Hawa<sup>45</sup> for the latter, respectively. It is very important to obtain positive values for  $(\gamma_S^+)^{1/2}$  and  $(\gamma_S^-)^{1/2}$  prior to the determination of  $\gamma_S^+$  and  $\gamma_S^-$ , otherwise one will be facing an anomaly.

It should be noted that applying this graphical approach to the contact angle data of Good and Hawa<sup>45</sup> yielded  $\gamma_S^+ = 0.1$  and  $\gamma_S^- = 9.2$  mJ/m<sup>2</sup>, comparable to the average values determined using the sets (water/ethylene glycol) and (water/formamide) published by these authors. The set (ethylene glycol/formamide) cannot be used here because these liquids have very comparable  $(\gamma_L^+/\gamma_L^-)^{1/2}$  values. To plot such graphs one obviously needs to have test liquids with very differing values of  $(\gamma_L^+/\gamma_L^-)^{1/2}$ . This is comparable to the situation occurring when Drago's  $E$  and  $C$  parameters for materials are to be determined using test probes with appreciably different  $C/E$  ratios.<sup>46</sup>

In the literature, sets of  $\gamma_S^+$  and  $\gamma_S^-$  are reported for each set of two liquids wetting the solid under investigation. Average values of  $\gamma_S^+$  and  $\gamma_S^-$  are then derived, and obviously we do prefer our graphical approach shown in Figure 3.

One of the reviewers raised the more general problem of determining acid–base characteristics of surfaces using the contact angle measurements approach of van Oss et al.<sup>36</sup> on the basis of the critique of Greiveldinger and Shanahan.<sup>47</sup> We are aware, of course, of this critique, but our simple graphical approach shows that the “inverted problem” of Greiveldinger and Shanahan<sup>47</sup> to determine the  $\gamma_L^+$  and  $\gamma_L^-$  of water after determining  $\gamma_S^d$ ,  $\gamma_S^+$ , and  $\gamma_S^-$  using the classical organic liquids in wettability measurements *cannot be rigorously tested*. The idea of these authors is interesting but should first be tested with some of the classical liquids (formamide, ethylene glycol, glycerol, etc.) to which one adds at least one liquid having a  $(\gamma_L^+/\gamma_L^-)^{1/2}$  ratio close to that of water ( $(\gamma_L^+/\gamma_L^-)^{1/2} = \gamma_L^+/\gamma_L^- = 1$ ). Figure 3 shows that depending on the choice of the organic liquids, one can end up with very different straight lines and thus very differing  $\gamma_S^+$  and  $\gamma_S^-$  values for the same solid surface and consequently “return” to  $\gamma_L^+$  and  $\gamma_L^-$  for water very much different from 25 mJ/m<sup>2</sup>. To date, and to our knowledge, no such ratio has been

(43) Costanzo, P. M.; Giese, R. F.; van Oss, C. J. *J. Adhes. Sci. Technol.* **1990**, *4*, 267.

(44) Chehimi, M. M.; Azioune, A.; Cabot-Deliry, E. In *Handbook of Adhesive Technology*; Mittal, K. L., Pizzi, A., Eds.; Dekker: New York, in press.

(45) Good, R. J.; A. K. Hawa, *J. Adhes.* **1997**, *63*, 5.

(46) Fowkes, F. M. *J. Adhes. Sci.* **1990**, *4*, 669.

(47) Greiveldinger, M.; Shanahan, M. E. R. *J. Colloid Interface Sci.* **1999**, *215*, 170.

**Table 3. Surface Free Energy Components for Polypyrrole Substrates and HSA**

	$\gamma$	$\gamma_s^d$	$\gamma_s^{AB}$	$\gamma_s^+$	$\gamma_s^-$
PPyCl <sup>a</sup>	46.6	36.6	6.9	0.427	28.27
	43.6		7.0	0.43	28.2
PPyDS <sup>a</sup>	41.7	34.8	6.9	1.35	8.85
	41.1		6.3	0.87	11.4
PPyTS <sup>a</sup>	36.5	31.6	5.0	4.26	1.45
	36.8		5.3	2.22	3.12
HSA <sup>b</sup>	41.4	41	0.4	0.002	20

<sup>a</sup> Upper values of  $\gamma_s^+$  and  $\gamma_s^-$  calculated from classical method based on two equations, and lower values calculated from Figure 3. <sup>b</sup> Data taken from ref 43.

found for the liquids for which the  $\gamma_L^+$  and  $\gamma_L^-$  values have been determined. The reader must be aware that here we mean values of  $\gamma_L^+$  and  $\gamma_L^-$  determined on the basis of  $\gamma_L^+ = \gamma_L^- = 25 \text{ mJ/m}^2$  for water.

In the case of PPyCl, diiodomethane and  $\alpha$ -bromonaphthalene spontaneously spread on the surface. Therefore, we relied on the contact angles of the bifunctional liquids water, glycerol, and formamide implemented in a system of three equations of the type (9) to determine the three unknown surface free energy components of PPyCl.

The values of  $\gamma_s^d$ ,  $\gamma_s^+$ , and  $\gamma_s^-$  for the three polypyrrole surfaces and HSA are reported in Table 3.

There are some interesting features about the  $\gamma_s^d$  (dispersive property),  $\gamma_s^+$  (acidity), and the  $\gamma_s^-$  (basicity) scales reported in Table 3: polypyrroles appear to have just as much surface energy as “polar” insulating organic materials, whereas using inverse gas chromatography (IGC), we have shown that polypyrrole behaves like metals and metal oxides; i.e., it is a high surface energy material.<sup>48</sup> However, IGC was applied at infinite dilution, that is, in a regime where molecular probes are injected at zero coverage. In this case, if the material under test is energetically heterogeneous, solutes will preferentially probe the high-energy sites and hence the high  $\gamma_s^d$  values determined by IGC for polypyrrole (up to 145 mJ/m<sup>2</sup> at 50 °C). This is why contact angle measurements and IGC at infinite dilution can lead to quite different results. As far as contact angle measurements are concerned, our  $\gamma_s^d$  value for PPyCl compares fairly well with that (35.8 mJ/m<sup>2</sup>) reported by Liu et al.<sup>41</sup>

If we consider now the acid–base properties of polypyrrole, the trends are as follows:

$$\gamma_s^+: \text{PPyTS} > \text{PPyDS} > \text{PPyCl}$$

$$\gamma_s^-: \text{PPyCl} > \text{PPyDS} > \text{PPyTS}$$

These trends show that PPyTS is more acidic than PPyCl. In contrast, the latter is more basic than the former. This is exactly what we have found using IGC a few years ago.<sup>49</sup> The intermediate values obtained for PPyDS may perhaps be due to the long dodecyl chain which induces moderate properties.

It is worth noting that, contrary to many surfaces, polypyrrole has a substantial acidic character, much stronger than that of the reference acidic insulating polymer PVC ( $\gamma_s^+ = 0.04$ <sup>39</sup> and 0.42<sup>50</sup> but can compare with the acidic character of glass, acid-washed glass, and native silica at the silicon surface ( $\gamma_s^+ = 1.97, 2.82$ , and

4 mJ/m<sup>2</sup>, respectively).<sup>51</sup> Despite the amphoteric behavior of polypyrrole, we found the  $\gamma_s^-$  values somehow small compared to typically basic surfaces such as PMMA,<sup>39,50</sup> has,<sup>43</sup> or aminosilane-treated glass.<sup>44</sup>

Table 3 and the acid–base characteristic trends discussed above clearly suggest that the most important property of polypyrrole when interacting with HSA is the Lewis acidity simply because the protein is fairly basic, thus leading to a strong acid–base PPy–HSA interaction. HSA is very poorly acidic and PPys are only mild bases so that the combination PPy–HSA (where PPy is the base and HSA the acid) will not promote the whole substrate–protein interaction.

**(4) Absolute Hydrophobicity and Hydrophobic Interfacial Polypyrrole–HSA Interactions.** The hydrophobic character of materials can be estimated in a semiquantitative manner by water contact angle or by measuring the uptake of water vapors. One can also use the VOGC theory to determine a scale of absolute hydrophobicity. The interfacial free energy between molecules of the compound (i) immersed in water  $\Delta G_{1W1}$  is the appropriate measure of hydrophilicity/hydrophobicity<sup>52</sup> and is expressed by

$$\Delta G_{1W1} = -2\gamma_{1W}$$

$$\Delta G_{1W1} = -2(\sqrt{\gamma_1^{LW}} - \sqrt{\gamma_W^{LW}})^2 - 4(\sqrt{\gamma_1^+ \gamma_1^-} + \sqrt{\gamma_W^+ \gamma_W^-} - \sqrt{\gamma_1^+ \gamma_W^-} - \sqrt{\gamma_1^- \gamma_W^+}) \quad (14)$$

According to van Oss,<sup>52</sup> when  $\Delta G_{1W1} > 0$ , the material immersed in water is considered hydrophilic, and when  $\Delta G_{1W1} < 0$ , it is hydrophobic. In general, the more  $\Delta G_{1W1}$  is negative, the more the material is hydrophobic. Hydrophilic particles ( $\Delta G_{1W1} > 0$ ) form stable suspensions in water, and under the same conditions hydrophilic molecules and macromolecules (such as HSA) are soluble. In contrast, hydrophobic particles clump together when immersed in water and molecules are insoluble.

The VOGC theory can further be used to determine the interfacial PPy–HSA (1–2) interaction energy in water (w):<sup>43</sup>

$$\Delta G_{1W2} = \gamma_{12} - \gamma_{1W} - \gamma_{2W} \quad (15)$$

where  $\gamma_{ij}$  is the interfacial tension between two materials. Equation 15 can be rewritten as a function of the surface tension components:

$$\Delta G_{1W2} = (\sqrt{\gamma_1^d} - \sqrt{\gamma_2^d})^2 - (\sqrt{\gamma_1^d} - \sqrt{\gamma_W^d})^2 - (\sqrt{\gamma_2^d} - \sqrt{\gamma_W^d})^2 + 2[\sqrt{\gamma_W^+}(\sqrt{\gamma_1^-} + \sqrt{\gamma_2^-} - \sqrt{\gamma_W^-}) + \sqrt{\gamma_W^-}(\sqrt{\gamma_1^+} + \sqrt{\gamma_2^+} - \sqrt{\gamma_W^+}) - \sqrt{\gamma_1^- \gamma_2^+} - \sqrt{\gamma_1^+ \gamma_2^-}] \quad (16)$$

Using the surface tensions components determined for PPyCl, PPyDS, PPyTS, HSA, and water in numerical applications of eqs 14 and 16, we determined  $\Delta G_{1W1}$  (absolute hydrophobicity) values for the substrates and  $\Delta G_{1W2}$  values for the various PPy–W–HSA systems (see Table 4).

The negative values of  $\Delta G_{1W2}$  indicate that the hydrophobic PPy–HSA interaction is attractive. More importantly, these values parallel the trends of HSA adsorption on one hand and either water static or receding contact angles on PPy surfaces on the other hand. Adsorption is

(48) Chehimi, M. M.; Abel, M. L.; Perruchot, C.; Delamar, M.; Lascelles, S. F.; Armes, S. P. *Synth. Met.* **1999**, *104*, 51.

(49) Chehimi, M. M.; Lascelles, S. F.; Armes, S. P. *Chromatographia* **1995**, *41*, 671.

(50) McCafferty, E.; Whightman, J. P. *J. Adhes. Sci. Technol.* **1999**, *13*, 1415.

(51) Freitas, A. M.; Sharma, M. M. *Langmuir* **1999**, *15*, 2499.

(52) van Oss, C. J. In *Acid–Base Interactions: Relevance to Adhesion Science and Technology*; Mittal, K. L., Ed.; 2000; Vol. 2, pp 173–179.



**Table 4.** Values of  $\Delta G_{1W1}$  and  $\Delta G_{1W2}$  (mJ/m<sup>2</sup>) Determined for PPyCl, PPyDS, and PPyTS Substrates and Their Relation with Protein Maximum Adsorption onto Polypyrrole Powders (mg/g)

materials	PPyTS	PPyDS	PPyCl
$\Delta G_{1W1}$ (mJ/m <sup>2</sup> )	47	35.31	+0.26
$\Delta G_{1W2}$ (mJ/m <sup>2</sup> )	46	29.6	7
HSA adsorption (mg/g)	70 ± 10	35 ± 5	25 ± 5

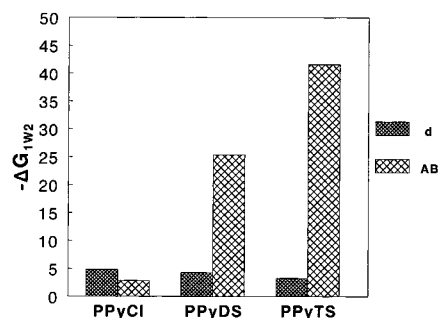
found also to definitely increase with the absolute hydrophobicity of the substrates. The hydrophobic character calculated for the polypyrrole powders is in line with the flocculation of these materials in water. In addition, hydrophilic species tend to be «monofunctional» donors with values of  $\gamma^- \geq 28.5$  mJ/m<sup>2</sup>.<sup>52</sup> In the present case, PPyCl has a  $\gamma^-$  of 28.2 mJ/m<sup>2</sup> and behaves as the most hydrophilic substrate, although it does flocculate. It can thus be considered as a borderline (between flocculation and suspension) polymeric species. This quantitative, relative hydrophilic character of PPyCl is responsible for the relative low HSA adsorption on its surface.

$\Delta G_{1W2}$  values were not split into enthalpic and entropic terms, but since hydrophobic interactions are shown to be important, possibly the entropy of adsorption has a substantial effect on the whole adsorption process.<sup>1</sup> Indeed, conformational changes of the HSA at the interface are likely to occur on the basis of our ongoing study of contact angle measurements of water drops onto HSA-coated polypyrrole at various coverage degrees.

We wanted to make one step beyond the  $\Delta G_{1W2}$  values reported in Table 4 by splitting them into their dispersive and acid–base contributions ( $\Delta G_{1W2}^d$  and  $\Delta G_{1W2}^{AB}$ , respectively), derived from eq 16. Figure 4 compares the dispersive and acid–base interactions at PPy–water–HSA for PPyCl, PPyDS, and PPyTS: there is strong supporting evidence for the very important role of Lewis acid–base forces to the hydrophobic conducting polymer–protein interaction, especially in the case of PPyTS.

### Conclusion

Adsorption of human serum albumin was carried out onto polypyrrole powders at pH 7.4. The plateau value (in the 25–70 mg/g range) depends on the nature of the polypyrrole dopant which induces a different structure of host polymer. Polypyrrole is thus a very strong bioad-

**Figure 4.** Dispersive (d) and acid–base (AB) contributions to the interfacial interaction energy between polypyrrole and human serum albumin immersed in water.

sorbent of proteins. The results were discussed in terms of hydrophilic/hydrophobic interactions. The use of electrochemically synthesized polypyrrole films as model surfaces are amenable to contact angle measurements of reference liquid drops. Water was used to qualitatively interrogate the hydrophobic character of polypyrroles, of which the decreasing trend was PPyTS > PPyDS > PPyCl. Using a more elegant method proposed and advocated by van Oss et al., the “absolute hydrophobicity” was calculated and its decreasing trend was that of water contact angles.

The interfacial interaction free energies ( $\Delta G_{1W2}$ ) of HSA and polypyrrole immersed in water, determined by the VOGC theory, were found to be negative, an indication that hydrophobic interactions between the host polymers and the protein are attractive. In addition, splitting  $\Delta G_{1W2}$  into its dispersive and acid–base interactions brought strong supporting evidence for the determinant role of acid–base interactions at the substrate–protein system immersed in water.

It is clear from this work that the VOGC theory is very useful for understanding the nature of interfacial interactions between human serum albumine and polypyrrole powders immersed in water.

**Acknowledgment.** The authors wish to thank the French EGIDE and the Polish Academy of Science for financial support through the Polonium scheme (Grant No. 98053).

LA0104440